
Performance analysis and enhancement of the performance of solar air heater using multiple ribs

Geetanjali Raghav

**University of Petroleum and Energy Studies, India*

Abstract.

The Industrial Revolution led to the establishment of additional industries, which in turn led to a rise in the usage of energy in the form of fossil fuels. Due to problems with the usage of fossil fuels, alternative forms of energy have gained importance and relevance in the modern era. These resources are said to as renewable since they, like the sun and wind, can never run out. They have a less carbon footprint and are additionally known as unconventional sources of energy. Thermal pollution can be considerably decreased. They have the potential to be inexhaustible, limitless sources of energy. The majority of renewable, polluted air energy sources are typically clean. Investigations have focused on the following things: The majority of renewable, pollution-free energy sources are typically clean. Researchers have studied the effects of the factors relative width distance (Gd/Lv), relative gap width (g/e), relative roughness height (e/D) and roughness width ratio (W/w),. The optimal rib hardness parameter values have indeed been reviewed and analyzed. Using experimentally obtained data, correlations for Nu & friction factor as functions of Re have been constructed. A multi-V-shaped rib with gap parameters has been investigated.

Keywords: solar air heater, ribs, heat transfer

1 INTRODUCTION

The thermal efficiency of the solar air heaters is enhanced by the rise in heat transfer area. Use of this type of heater was advised by Lof et al, having an advantage of negligible pressure loss and is quite effective for a slight temperature increase. However, the price of the device increases because to the demand for a huge glass surface. As a result, it is preferable for turbulence to be generated only in the viscous sub-layer region, which is where thermal resistance occurs, which is located close to the absorber. Artificial roughness is surface texture that has been produced artificially. This can be accomplished by identifying ribs in various configurations, such as hill transverse, inclined, V-shaped, multi-V, or W ribs. These researchers looked at how heat transmission and friction factor in applications for cooling gas turbines and heat exchangers were affected by geometric characteristics of roughness element Momin and others (2002 For a fixed relative roughness of 10 and a Reynolds number range of 2500- 18000, the effects of relative roughness height and angle of attack were experimentally explored. The impact of V-shaped rib array on the friction and heat transfer of fully developed flows in a square channel was studied by Lau et al. in 1991. In order to predict the impact of the rib heads chamfer angle inside a rectangular channel with integral chamfered ribs, Karwa et al. (1999) conducted an experimental analysis. Ahu et al (2005) carried out an experimental analysis of a comparable geometry with broken transverse ribs for solar air heaters. Aspect ratio of 8, roughness height of 10–30 mm, height of the ribs of 1.5 mm, and Reynolds number variation of 3000–12,000 were the factors that the experiment examined. Regular imperfection geometries that can be created as voids and ribs were studied by Donne and Meyer [7, 8]. Transverse rib roughness was the focus of earlier studies on rib smoothness by Webb et al. In a different study, Prasad and Saini [10] used circular wires to artificially roughen the heated plate's inner surface. They claimed that there had been a considerable improvement in the heat transfer coefficient. The ideal values for the rib roughness parameter have been determined and discussed. Using experimentally obtained data, correlations for Nu and f as functions of Re have been developed. A multi-V-shaped rib with gap parameters has been investigated.

2. METHODOLOGY

The appropriate values or range of values for all pertinent parameters for the collector system, categorized into fixed and variable parameters. With an objective of the investigating the exergetic performance of the solar air heater for a given set of system and operating parameters.

Table 2.1: System and operating parameters

System parameter	Fixed	Parameter	Value/Range
		Collector length (L), m	2
Collector width (W), m	1		
Duct depth (H), m	0.025		
Thickness of collector plate (t_p), m	0.002		
Number of glass covers (N)	1		
Thermal conductivity of insulation (k_i), W/m-K	0.037		
Thickness of insulation (δ_i), m	0.05		
Transmittance-Absorptance product ($\eta\alpha$)	0.80		
Emissivity of the absorber plate (ϵ_p)	0.90		
Emissivity of the glass cover (ϵ_g)	0.88		
Thickness of glass cover (t_g), m	0.004		
Air gap between absorber plate and glass cover (L_{ag}), m	0.025		
Thickness of collector edge (t_e), m	0.1		
Slope of collector (β), degree	43		
Variable	Relative roughness height (e/D_h)	0.019-0.043	
	Relative roughness pitch (p/e)	3-8	
	Flow angle of attack (α), degree	30-75	
	Relative roughness width (W/w)	1-10	
Operating parameter	Fixed	Ambient temperature (T_a), K	300
		Wind velocity (V_w), m/s	1
Variable	Temperature rise parameter ($\Delta T/I$), K-m ² /W	0.002-0.025	
	Solar radiation intensity (I), W/m ²	600-1000	

2.1 Procedure for evaluation of exergetic Components and Exergetic Performance:

The solar air heating is assumed to suck in surrounding atmosphere for the purposes of this study, producing input air that is the same temperature as the surrounding. The projected global temperature of the air passing through the duct (T) and the entrance air temperature are used to compute the output air temperature.

$$T_o = T_i + \Delta T$$

Mean film temperature (T_{fm})

$$T_{fm} = \frac{T_i + T_o}{2}$$

Now from the value of mean film temperature, average and estimated initial mean plate temperature is presumed

$$T_{pm} = T_{fm} + 10$$

The Mullick et al [85] equation;

$$U_t = \left[\left\{ \frac{12.75((T_{pm}-T_c) \cos \beta)^{0.264}}{(T_{pm}+T_c)^{0.46} L_s^{0.21}} + \frac{\sigma(T_{pm}^2+T_c^2)(T_{pm}+T_c)}{\frac{1}{\epsilon_p} + \frac{1}{\epsilon_c} - 1}} \right\}^{-1} + \left\{ h_w + \frac{\sigma \epsilon_c (T_c^4 - T_s^4)}{(T_c - T_a)} \right\}^{-1} + \frac{t_g}{k_g} \right]^{-1}$$

Back loss coefficient U_b , is expressed as,

$$U_b = \frac{K_i}{\delta_i}$$

Table 2.2: Estimation of the thermal performance

Parameter	Formula
Thermal efficiency	$\eta_{th} = Q_u/A_p I$
Effective efficiency	$\eta_{eff} = \frac{Q_u - \frac{P_m}{c}}{A_p I}$
Absolute or net Exergy flow	$E_n^* = IA_p \eta_{th} \eta_c - P_m (1 - \eta_c)$
Carnot Efficiency	$\eta_c = 1 - \frac{T_a}{T_{im}}$
Exergy inflow	$E_s^* = A_p I \eta_{ex} = IA_p \left(1 - \frac{T_a}{T_{sun}}\right)$
Exergetic efficiency	$\eta_{II} = \frac{E_n^*}{E_s^*}$
Optical exergy	$E_{LO}^* = IA_p \eta_{ex} (1 - \tau \alpha)$

3. RESULTS AND DISCUSSION

3.1 Impact of relative roughness height, pitch, and width ratio on exergy loss components:

For different system (flow angle of attack) and operational parameter values, the exergetic components of a solar air heater with multiple purposefully roughened V-ribs have been found. The appropriate roughness parameter values (angle of attack) that will result in the best exergetic performance from a solar air heater have been identified. The following exergy losses components are explored individually:

3.1.1 Optical Exergy Losses (\dot{E}_{LO})

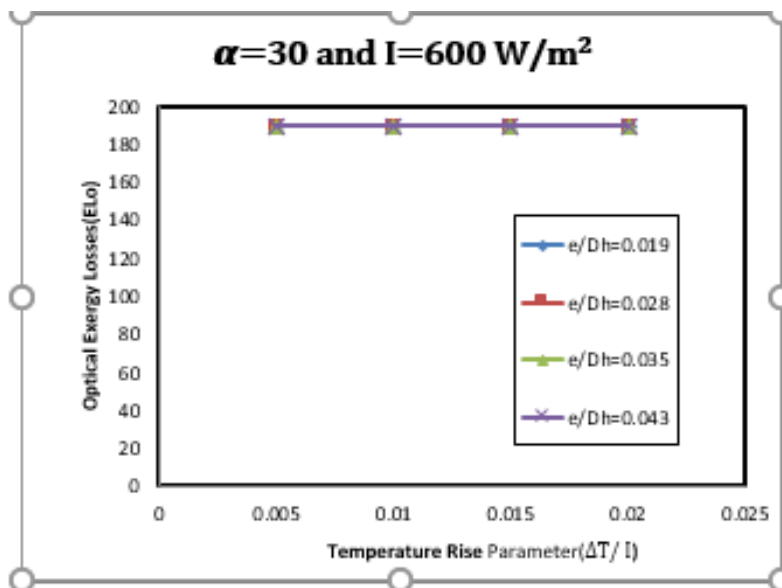


Fig 3.1 Variation of energy losses (optical)

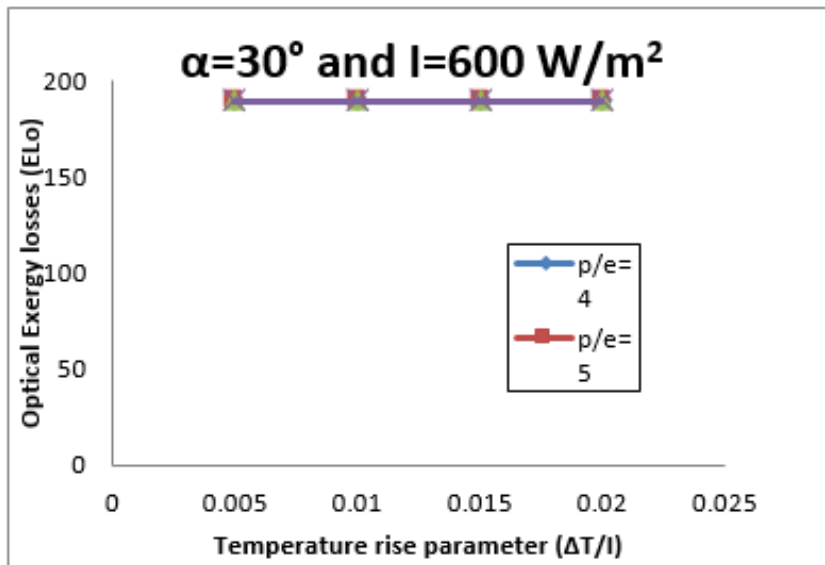


Fig. 3.2 Effect of temperature rise on energy losses

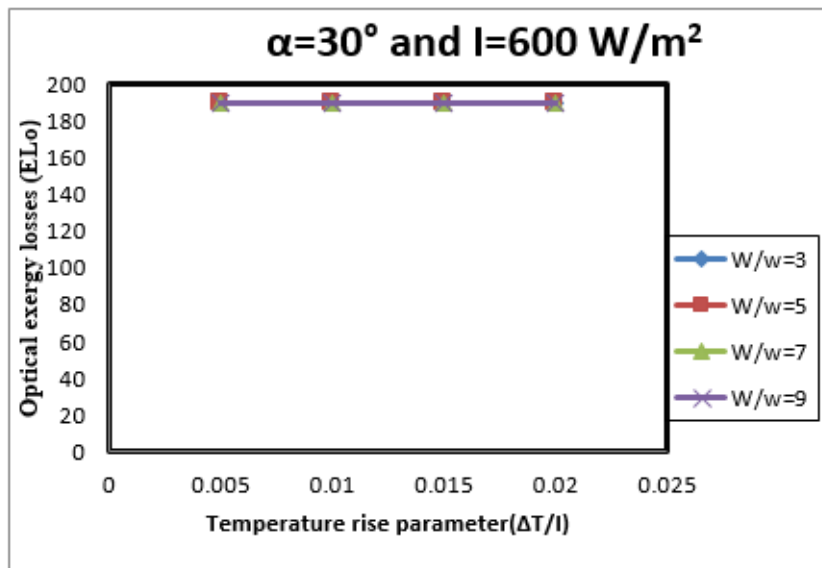


Fig.3.3 Variation of E_{Lo} with temperature rise parameter ($\Delta T/I$) for different (W/w).

For given values of various roughness as well as operating parameters, Figs. 3.1, 3.2, and 3.3 demonstrate that the optical exergy inefficiencies are independent of the temperature rise factor (T/I), comparative roughness height (e/Dh), relative roughness pitch (p/e), & relative roughness width ratio. That's because the energy destroyed as a result of the cover's transmission and the importer plate's assimilation is independent of both the temperature of the cover and the absorber plate and only rely on the transmittance – absorptance ($\alpha\tau$) product, which has been anticipated to be constant.

3.2.2 Exergy loss occur due to the absorber's irradiation during assimilation (\dot{E}_{LA}):

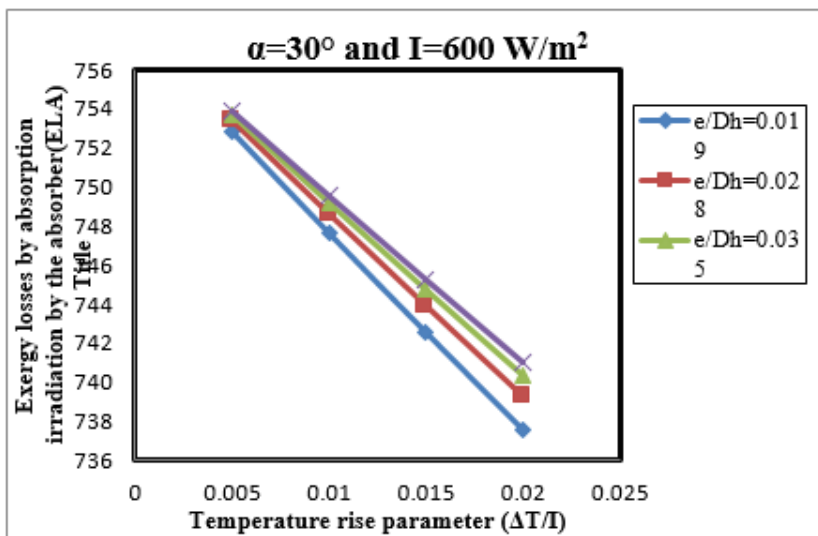


Fig .3.4 Variation of ELA with temperature rise parameter($\Delta T/I$) for different(e/Dh).

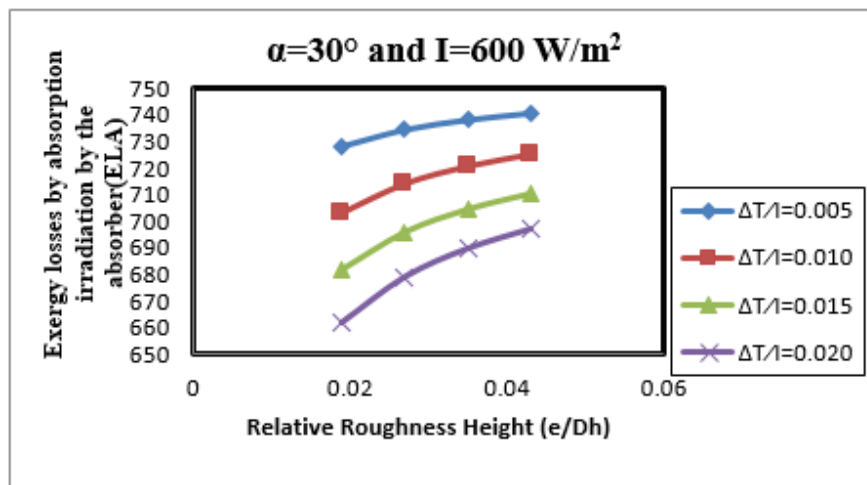


Fig .3.5 Variation of ELA with Relative roughness Hight (e/Dh) for different($\Delta T/I$)

As shown in Figs. 3.4 and 3.5, At mean sheet temperature T_{pm} , the absorber's Radiation exposure absorption accounts for the majority of energy losses; the value decreases as the temperature rise parameter (T/I) is raised. It exhibits the greatest losses at the lowest temperature rise parameter value ($T/I=0.005$) and the smallest losses at the highest temperature rise parameter value ($T/I=0.025$). Additionally, the relative roughness height has an impact, with an increase in relative roughness height leading to an increase in exergy losses. Since energy at higher temperatures implies bigger amounts of exergy, a high absorber temperature reduces exergy losses through absorption. A higher absorber plate temperature and, hence, more energy are created for a similar amount of absorbed energy when the "roughness height" parameter is set to 1.

4. Conclusion

The effectiveness of a solar-powered air heater with multiple V rib shape that has been artificially roughened has been investigated using a mathematical modelling technique. Studies have been done on how system and operating characteristics affect different energy component types. The amount of energy lost during the transfer of heat from the absorber dish to the working medium increases with the temperature rise parameter, decreases with the ratio of relative looking to upgrade, pitch, and breadth, and is at its lowest value at an angle of attack of 60 degrees. As the temperature rise factor grows, the energetic efficiency of the collector rises as well. However, excessively low values

of this factor may provide a negative result because of the heat transfer process that takes place between the absorber surface and medium

REFERENCES

- [1] Prasad, B.N., Saini, J.S., 1988. Effect of artificial roughness on heat transfer and friction factor in a solar air heater. *Solar Energy* 41 (6), 555–560.
- [2] Gupta, D., Solanki, S.C., Saini, J.S., 1993. Heat and fluid flow in rectangular solar air heater ducts having transverse rib roughness on absorber plates. *Solar Energy* 51, 31–37.
- [3] Bhagoria, J.L., Saini, J.S., Solanki, S.C., 2002. Heat transfer coefficient and friction factor correlations for rectangular solar air heater duct having transverse wedge shaped rib roughness on the absorber plate. *Renewable Energy* 25, 341–369.
- [4] Karwa, R., Solanki, S.C., Saini, J.S., 1999. Heat transfer coefficient and friction factor correlations for the transitional flow regime in rib roughened rectangular ducts. *International Journal of Heat and Mass Transfer* 42, 1597–1615.
- [5] Momin, A.-M.E., Saini, J.S., Solanki, S.C., 2002. Heat transfer and friction in solar air heater duct with V-shaped rib roughness on absorber plate. *International Journal of Heat and Mass Transfer* 45, 3383–3396.
- [6] Muluwork, K.B., Saini, J.S., Solanki, S.C., 1998. Studies on discrete RIB roughened solar air heaters. In: *Proceedings of National Solar Energy Convention, Roorkee*; pp. 75– 84.
- [7] Jaurker, A.R., Saini, J.S., Gandhi, B.K., 2006. Heat transfer and friction characteristics of rectangular solar air heater duct using rib-grooved artificial roughness. *Solar Energy* 80 (8), 895–907.
- [8] Sahu, M.M., Bhagoria, J.L., 2005. Augmentation of heat transfer coefficient by using 90° broken transverse ribs on absorber plate of solar air heater. *Renewable Energy* 30, 2057– 2063.
- [9] Saini, R.P., Saini, J.S., 1997. Heat transfer and friction factor correlations for artificially roughened ducts with expanded metal mesh as roughened element. *International Journal of Heat and Mass Transfer* 40 (4), 973–986.

